Quantum phases of bosons in double-well optical lattices

I. Danshita,[1,2] J. E. Williams,[3] C. A. R. Sá de Melo,[1,4] and C. W. Clark[1]

[1]*Joint Quantum Institute, National Institute of Standards and Technology and University of Maryland,*
Gaithersburg, Maryland 20899, USA
[2]*Department of Physics, Waseda University, 3-4-1 Ōkubo, Shinjuku, Tokyo 169-8555, Japan*
[3]*Wolfram Research, Inc., Champaign, Illinois 61820, USA*
[4]*School of Physics, Georgia Institute of Technology, Atlanta, Georgia 30332, USA*

We study the superfluid and insulating phases of bosons in double-well optical lattices, and focus on the specific example of a two-legged ladder, which is currently accessible in experiments. We obtain the zero-temperature phase diagram using both mean-field and time-evolving block decimation techniques. We find that the mean-field approach describes the correct phase boundaries only when the intrachain hopping is sufficiently small in comparison to the on-site repulsion. We show the dependence of the phase diagram on the interchain hopping or tilt between double wells. We find that the Mott-insulator phase at unit filling exhibits a nonmonotonic behavior as a function of the tilt parameter, producing a reentrant phase transition between Mott insulator and superfluid phases. Finally, we determine the critical point separating the insulating and superfluid phases at commensurate fillings, where the Berezinskii-Kosterlitz-Thouless transition occurs.

I. INTRODUCTION

Optical lattices loaded with ultracold atoms provide the opportunity to study quantum phases of many-particle systems because of their unprecedented degree of controllability [1]. At present, the lattice depth, dimensionality, geometry, and filling factor can all be reasonably controlled. While one of the first examples of this degree of control was the experimental observation of the superfluid (SF)–to–Mott insulator (MI) transition in three-dimensional cubic optical lattices as a function of the lattice depth [2], tetragonal and orthorhombic optical lattices can also be produced by deepening the optical potential along desired directions [3,4].

More recently, possibilities for control have expanded with the experimental realization of double-well optical lattices. Control of the polarization of the laser beams allows for the production of lattices with a base in two and three dimensions [5] as illustrated in Fig. 1(a), where Bose atoms (^{87}Rb) have been successfully trapped. In particular, one can create a one-dimensional double-well optical lattice corresponding to the two-leg ladder structure shown in Fig. 1(b) by increasing the long period of the double-well optical lattice. In standard condensed-matter physics, a few compounds, such as vanadyl pyrophosphate $(VO)_2P_2O_7$ [6] and some cuprates like $SrCu_2O_3$ [7], have such two-leg ladders in their crystalline structure, and they display much of the interesting physics encountered in general ladder systems, associated with the interplay between spin-gapped and superconducting states [8]. However, conventional condensed-matter systems come with fixed dynamical and structural parameters, while the flexible variability of optical lattices offers the prospect of exploring the full parameter space. Moreover, the particles confined in the current double-well optical lattices are bosonic atoms, in contrast to conventional condensed-matter systems, where electrons (fermions) dictate the quantum phases.

In this paper, we study the zero-temperature phase diagram of bosons in double-well optical lattices and focus on

the case of a two-legged ladder, where analytical and numerical progress can be made. In particular, we apply the time-evolving block decimation (TEBD) method [9,10] to such ladder systems, which are experimentally accessible [5], and discuss the SF-to-MI transition, which is expected to be observed in future experiments.

Our main results are as follows. We show that the phase diagram changes dramatically as a function of the chemical potential μ, the intrachain hopping $t_\parallel$, the interchain hopping $t_\perp$, the on-site repulsion U, and the tilt λ of the double well, which are indicated in Figs. 1(b) and 1(c). For $\lambda=0$ and different ratios $t_\perp/U$, Mott phases with half-integer (in addition to integer) filling factors emerge in the phase diagram of μ/U versus $t_\parallel/U$ for small ratios of $t_\parallel/U$. As $t_\perp/U$ increases, the half-filling MI phase becomes larger and the unit-filling one becomes smaller. For fixed ratio $t_\perp/U$ and different values of λ/U, we also obtain the μ/U versus $t_\parallel/U$ phase diagram, which reveals a reentrant phase transition for the unit-filling MI induced by the tilt λ. The reentrant phase transition can be attributed to the development of coherence in each
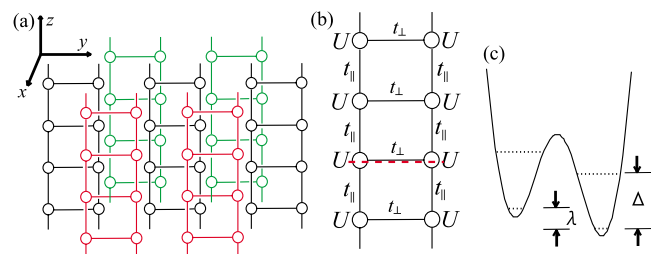
FIG. 1. (Color online) (a) Schematic picture of a three-dimensional (3D) configuration of a double-well lattice. Circles represent sites, and solid lines represent connections via the hopping between sites. (b) Schematic picture of the two-leg ladder. (c) Double-well potential corresponding to the cross section for the dashed line in (b). Dotted lines represent the energy levels for each well.

double well in the vicinity of $\lambda = U$, which drives the system into the SF phase. Finally, for half and unit fillings, we calculate the critical points corresponding to a Berezinskii-Kosterlitz-Thouless (BKT) transition at the MI-to-SF phase boundary.

The remainder of the paper is organized as follows. In Sec. II, we introduce our model Hamiltonian describing bosons in a two-legged optical lattice. In Sec. III, we restrict ourselves to the limit where the intrachain hopping $t_\parallel$ is zero, and discuss the MI phases. In Sec. IV A, we calculate analytically the phase boundary of the SF-to-MI transition within the perturbative mean-field approach (PMFA). In Sec. IV B, we use the TEBD method to obtain numerically the correct phase boundaries where the PMFA fails. In addition, we compute the critical points separating the insulating and superfluid phases at commensurate fillings, where the BKT transition occurs. Last, in Sec. V, we summarize our results and present our main conclusions.

II. MODEL

The basic physics of interacting bosons in an optical lattice can be described by the Bose-Hubbard model [1,11]. We introduce the Bose-Hubbard model for the double-well ladder

$$H = \sum_i \left(H_i^{\mathrm{dw}} - t_\parallel \sum_{\eta \in \{L,R\}} (a_{i+1,\eta}^\dagger a_{i,\eta} + \mathrm{H.c.}) \right), \qquad (1)$$

where H_i^{dw} represents the double-well Hamiltonian for a given ladder index i and is given by

$$H_i^{\mathrm{dw}} = \sum_\eta \left(\frac{U}{2} \hat{n}_{i,\eta}(\hat{n}_{i,\eta} - 1) - \mu \hat{n}_{i,\eta} \right) - t_\perp (a_{i,R}^\dagger a_{i,L} + \mathrm{H.c.})$$

$$+ \frac{\lambda}{2} (\hat{n}_{i,L} - \hat{n}_{i,R}). \qquad (2)$$

$a_{i,\eta}^\dagger$ creates a boson at the lowest level localized on the left (right) of the ith double well when $\eta = L(R)$. A schematic picture of the Bose-Hubbard model for the double-well ladder is shown in Figs. 1(b) and 1(c). We assume that all parameters are sufficiently small compared to the energy gap Δ between the first and second levels of each site, and we do not include the effect of the harmonic trapping potential. Furthermore, all parameters of H are controllable in experiments [5], and thus we begin our discussion by analyzing the limit of $t_\parallel = 0$.

III. INTEGER AND HALF-INTEGER MOTT PHASES

When $t_\parallel = 0$, several MI phases emerge. In this case, the Hamiltonian Eq. (1) reduces to $H = \Sigma_i H_i^{\mathrm{dw}}$. One can obtain the eigenenergy $E^{(0)}(n,j)$ and eigenstate

$$|\Phi_{n,j}\rangle = \sum_{n_L=0}^{n} C_{n_L}(n,j) |n_L, n - n_L\rangle$$

of H_i^{dw}, where n is the number of atoms in each double well and the quantum number j is a non-negative integer less than $n+1$ ($j = 0, 1, \ldots, n$). $|n_L, n_R\rangle$ is the Fock state with n_L (n_R)

atoms on the left (right) of each double well. The state $|\Phi_{n,0}\rangle$ is the ground state of H_i^{dw} with energy $E^{(0)}(n,0)$, when the following conditions are satisfied: $E^{(0)}(n+1,0) > E^{(0)}(n,0)$ and $E^{(0)}(n-1,0) > E^{(0)}(n,0)$. When n is even (odd), the filling factor ν of the MI phases is integer (half integer). The existence of half-integer-filling MI phases has also been noticed in Monte Carlo simulations and in cell strong-coupling perturbative techniques [12] for two-legged ladders with zero tilt and fixed ratio $t_\parallel / t_\perp$. Here, however, we use different methods and consider also the cases of finite tilt and independent hopping parameters. Although there exists a MI phase for each value of n, we focus here only on the half- and unit-filling MI phases ($\nu = 1/2, 1$).

We consider first the case of symmetric double wells ($\lambda = 0$) and discuss two limiting situations corresponding to (a) $t_\perp \ll U$ and (b) $t_\perp \gg U$.

(a) For $t_\perp \ll U$, the ground state is $|\Phi_{1,0}\rangle$ ($\nu = 1/2$) when the chemical potential satisfies the condition

$$-t_\perp < \mu < t_\perp + O\left(\frac{t_\perp^2}{U}\right), \qquad (3)$$

and the width of the half-filling MI phase on the μ line is $\sim 2t_\perp$. In the strict limit of $t_\perp = 0$, the half-filling MI phase vanishes and the system is always a superfluid since there is a low-energy path for the bosons to move along the chains. The ground state switches to $|\Phi_{2,0}\rangle$ ($\nu = 1$) when the chemical potential satisfies the condition

$$t_\perp + O\left(\frac{t_\perp^2}{U}\right) < \mu < U - 2t_\perp + O\left(\frac{t_\perp^2}{U}\right), \qquad (4)$$

and the width of the unit-filling MI phase becomes $\sim U$. As the interchain hopping $t_\perp$ vanishes, the unit-filling MI phase approaches that of a 1D lattice (two independent filling-1 chains).

(b) For $t_\perp \gg U$, the antibonding single-particle state of the double well is pushed to energies much higher than U, and only the bonding single-particle state and the lowest-energy two-particle state are important. Therefore, the $\nu = 1/2$ ($\nu = 1$) MI phase can be mapped into the unit- (double-)filling MI phase for a 1D lattice with an effective hopping $t_\parallel$ and an on-site repulsive interaction $U/2$. The ground state is $|\Phi_{1,0}\rangle$ ($\nu = 1/2$) when the chemical potential satisfies the condition

$$-t_\perp < \mu < -t_\perp + \frac{U}{2} + O\left(\frac{U^2}{t_\perp}\right). \qquad (5)$$

The ground state switches to $|\Phi_{2,0}\rangle$ ($\nu = 1$) when the chemical potential satisfies the condition

$$-t_\perp + \frac{U}{2} + O\left(\frac{U^2}{t_\perp}\right) < \mu < -t_\perp + U + O\left(\frac{U^2}{t_\perp}\right). \qquad (6)$$

From Eqs. (5) and (6), we can see that the width of both MI phases along the μ line is $\sim U/2$.

Next, we consider the case of tilted double wells, where $\lambda \neq 0$. The insulating states present in the double-well ladders discussed here are quite different from those encountered in strictly 1D superlattices [13–15]. When $\lambda \gg \max(t_\perp, U)$, the MI with filling ν in the double-well ladder

reduces to the MI with 2ν in a single 1D lattice. Even in this regime, a transition to a SF phase occurs at a certain critical value of the intrachain hopping $t_\parallel$, in contrast to the case of the 1D superlattice, where all the occupied wells are completely isolated from each other and the system remains always in the insulating phase.

We discuss two special cases, (a) $\lambda = U$ with $t_\perp \ll U$ and (b) $\lambda \gg \max(t_\perp, U)$.

(a) For $\lambda = U$ and $t_\perp \ll U$, where the states $|1,1\rangle$ and $|0,2\rangle$ are nearly degenerate, the ground state is $|\Phi_{1,0}\rangle$ ($\nu = 1/2$) when the chemical potential satisfies the condition

$$-\frac{U}{2} + O\left(\frac{t_\perp^2}{U}\right) < \mu < \frac{U}{2} - \sqrt{2}t_\perp + O\left(\frac{t_\perp^2}{U}\right). \quad (7)$$

The width of the half-filling MI phase on the μ line is $\sim U$. On the other hand, the ground state is $|\Phi_{2,0}\rangle$ ($\nu = 1$) when the chemical potential satisfies the condition

$$\frac{U}{2} - \sqrt{2}t_\perp + O\left(\frac{t_\perp^2}{U}\right) < \mu < \frac{U}{2} + \sqrt{2}t_\perp + O\left(\frac{t_\perp^2}{U}\right). \quad (8)$$

Thus, the width of the unit-filling MI phase is reduced to $\sim 2\sqrt{2}t_\perp$.

(b) For $\lambda \gg \max(t_\perp, U)$, the ground state is $|\Phi_{1,0}\rangle$ ($\nu = 1/2$) when the chemical potential satisfies the condition

$$-\frac{\lambda}{2} + O\left(\frac{t_\perp^2}{\lambda}\right) < \mu < -\frac{\lambda}{2} + U + O\left(\frac{t_\perp^2}{\lambda}\right). \quad (9)$$

The ground state is $|\Phi_{2,0}\rangle$ ($\nu = 1$) when the chemical potential satisfies the condition

$$-\frac{\lambda}{2} + U + O\left(\frac{t_\perp^2}{\lambda}\right) < \mu < -\frac{\lambda}{2} + 2U + O\left(\frac{t_\perp^2}{\lambda}\right). \quad (10)$$

From Eqs. (9) and (10), we can see that the width of both MI phases along the μ line is $\sim U$. This happens because the half- and unit-filling MI phases in a double-well ladder reduce to the unit- and double-filling MI phases of a single 1D lattice, as all bosons prefer to be in the lower-energy side of the greatly tilted double well.

These special cases reflect the more general trend that, as λ increases, the width of the unit-filling MI phase on the μ line changes nonmonotonically. Such nonmonotonic behavior for the unit-filling MI phase is also found in $(\mu, t_\parallel)$ plane for varying values of λ, and is discussed next by taking into account finite $t_\parallel$ to study the insulator-to-superfluid transition.

IV. INSULATOR TO SUPERFLUID TRANSITION

A. PMFA

In order to include the effects of the intrachain hopping $t_\parallel$ and study the MI-SF transition, we use first a perturbative mean-field approach [16]. Although the PMFA fails to describe 1D systems quantitatively [17], it provides qualitative understanding and analytical insight. The discussion of quantitative results is postponed to Sec. IV B, where we use the TEBD method [9,10] and compare its results with the picture that emerges from the PMFA.

We consider the effects of finite $t_\parallel$ and introduce the SF order parameter $\psi_\eta = \langle a_{i,\eta}\rangle = \langle a_{i,\eta}^\dagger\rangle$ into the Hamiltonian Eq. (1), which reduces to

$$H \simeq \sum_i H_i^{\mathrm{mf}} = \sum_i \left(H_i^{\mathrm{dw}} + 2t_\parallel \sum_\eta \psi_\eta^2 + V_i\right), \quad (11)$$

where $V_i = -2t_\parallel \sum_\eta \psi_\eta (a_i^\dagger + a_i)$ describes the transfer of atoms between the ith site and the condensate ψ_η and is treated perturbatively.

Using perturbation theory, we obtain the correction $\Delta E_n = E_n - E^{(0)}(n,0)$ to the unperturbed ground state energy $E^{(0)}(n,0)$ in terms of ψ_η. Performing a linear transformation $(\Psi_1, \Psi_2)^{\mathrm{t}} = X(\psi_L, \psi_R)^{\mathrm{t}}$ to diagonalize the quadratic part of ΔE_n leads to

$$\Delta E_n = \sum_{\zeta \in \{1,2\}} A_\zeta(n, \bar{t}_\perp, \bar{t}_\parallel, \bar{\mu})\Psi_\zeta^2 + O(\Psi_1^4, \Psi_1^3\Psi_2, \dots), \quad (12)$$

where X is a 2×2 Hermitian matrix and the overbars on parameters mean normalization by U, e.g., $\bar{\mu} \equiv \mu/U$. The expressions for the coefficients of Ψ_ζ^2 and fourth-order terms are quite long; thus we will not give them here. However, A_2 is always positive, while A_1 changes sign, and the fourth-order coefficients are positive, leading to second-order phase transitions between the MI ($\Psi_1 = \Psi_2 = 0$) and SF ($\Psi_1 \neq 0, \Psi_2 = 0$) states.

For symmetric double wells ($\lambda = 0$), we obtain analytical expressions for the MI-SF phase boundary ($A_1 = 0$) in the limits (a) $t_\perp \ll U$ and (b) $t_\perp \gg U$.

(a) When $t_\perp \ll U$, the phase boundaries in the $(\mu, t_\parallel)$ plane are obtained by expressing the intrachain hopping $t_\parallel$ in terms of the chemical potential μ and the interchain hopping $t_\perp$ as

$$\bar{t}_\parallel^{\mathrm{pb}} \simeq \begin{cases} \dfrac{\bar{t}_\perp^2 - \bar{\mu}^2}{4\bar{t}_\perp}, & n = 1 \quad (\nu = 1/2), \\[2ex] \dfrac{(\bar{\mu} - \bar{t}_\perp)(-\bar{\mu} + 1 - 2\bar{t}_\perp)}{2(\bar{\mu} + 1)}, & n = 2 \quad (\nu = 1). \end{cases} \quad (13)$$

In this case, the critical values of $t_\parallel$ for half and unit filling are given by

$$t_\parallel^{\mathrm{c}} \simeq \begin{cases} \dfrac{1}{4}t_\perp, & n = 1 \quad (\nu = 1/2), \\[2ex] \dfrac{3 - 2\sqrt{2}}{2}U - \dfrac{1}{2}t_\perp, & n = 2 \quad (\nu = 1), \end{cases} \quad (14)$$

with $\mu_c \simeq 0$ for $\nu = 1/2$ and $\mu_c \simeq (\sqrt{2} - 1)U$ for $\nu = 1$.

(b) When $t_\perp \gg U$, the double-well system reduces effectively to a single 1D lattice, and the phase boundaries as well as the value $t_\parallel^{\mathrm{c}}$ can be obtained from the standard results [16] by replacing $U \to U/2$ and $\mu \to \mu + t_\perp$. Therefore, the phase boundaries are given by
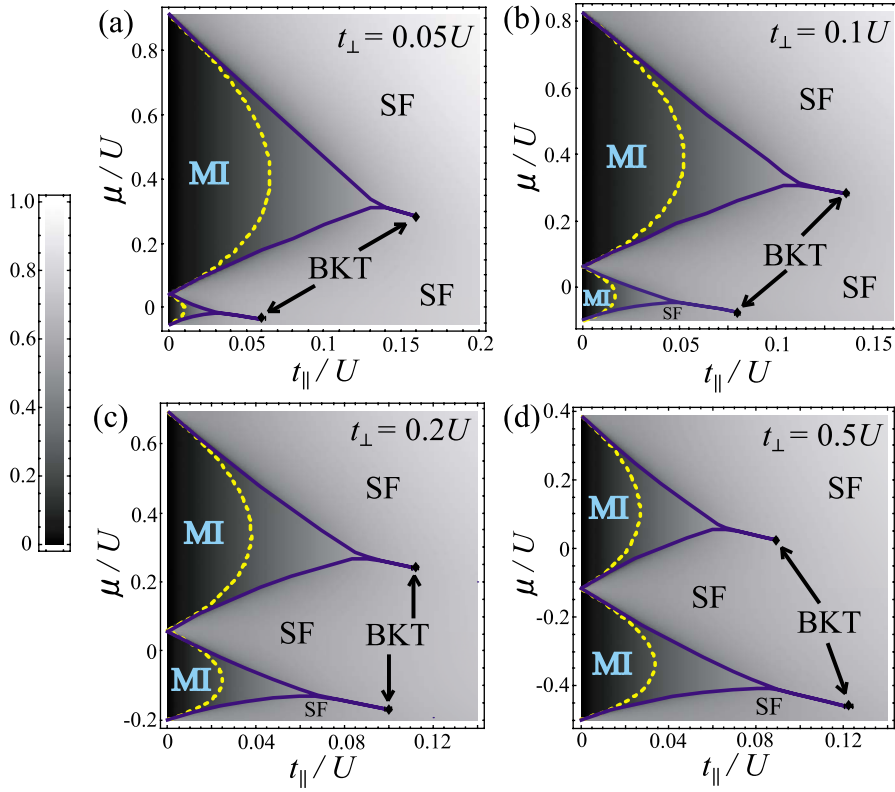
FIG. 2. (Color online) Phase diagrams for symmetric double wells ($\lambda=0$). Dashed lines represent the phase boundary calculated within the PMFA. Solid lines, density plots, and dots are calculated by the infinite TEBD method. $\tilde{n}$ is integer inside the solid lines. The density plots represent σ. The dots represent the critical points of the BKT transition.

$$\bar{t}_{\parallel}^{pb} \simeq \begin{cases} \dfrac{(\bar{\mu}+\bar{t}_{\perp})(-\bar{\mu}-\bar{t}_{\perp}+1/2)}{2(\bar{\mu}+\bar{t}_{\perp}+1/2)}, & n=1 \quad (\nu=1/2), \\[3mm] \dfrac{(\bar{\mu}+\bar{t}_{\perp}-1/2)(-\bar{\mu}-\bar{t}_{\perp}+1)}{2(\bar{\mu}+\bar{t}_{\perp}+1/2)}, & n=2 \quad (\nu=1). \end{cases} \tag{15}$$

For the half- and unit-filling cases, the critical values of $t_{\parallel}$ as a function of U are

$$t_{\parallel}^{c} \simeq \begin{cases} \dfrac{3-2\sqrt{2}}{4}U, & n=1 \quad (\nu=1/2), \\[3mm] \dfrac{5-2\sqrt{6}}{4}U, & n=2 \quad (\nu=1), \end{cases} \tag{16}$$

while the corresponding critical values of the chemical potential are given by

$$\mu_{c} \simeq \begin{cases} -t_{\perp} + \dfrac{\sqrt{2}-1}{2}U, & n=1 \quad (\nu=1/2), \\[3mm] -t_{\perp} + \dfrac{\sqrt{6}-1}{2}U, & n=2 \quad (\nu=1). \end{cases} \tag{17}$$

In Fig. 2, the MI-SF phase boundaries for $\lambda=0$ calculated within the PMFA are shown as dashed lines for different values of $t_{\perp}$. Notice that the figures are not on the same scale. In Fig. 3, the critical intrachain hoppings $t_{\parallel}^{c}$ for the half- and unit-filling MI phases are shown as functions of $t_{\perp}$ as dashed and solid lines. As the interchain hopping $t_{\perp}$ increases, the half-filling MI lobe or $t_{\parallel}^{c}$ grows and the unit-filling MI lobe or $t_{\parallel}^{c}$ shrinks, so that the double-well system

reduces to a single 1D system in the limit of $t_{\perp} \gg U$.

Next, we discuss the case of tilted double wells ($\lambda \neq 0$). In Fig. 4, we show the MI-SF phase boundaries for different values of λ at fixed $t_{\perp}=0.1U$ indicated by dashed lines. In Fig. 5, we show the critical intrachain hoppings $t_{\parallel}^{c}$ versus λ for the half- and unit-filling MI phases indicated by dashed and solid lines, respectively. The half-filling MI lobe or $t_{\parallel}^{c}$ grows monotonically as λ increases. In contrast, the unit-filling MI lobe or $t_{\parallel}^{c}$ changes nonmonotonically as a function of λ.

This nonmonotonic behavior for $\nu=1$ can be understood as follows. At $\lambda=0$, the critical intrachain hopping $t_{\parallel}^{c}$ is given approximately by Eq. (14) since $t_{\perp} \ll U$ when $t_{\perp}=0.1U$. As λ increases, $t_{\parallel}^{c}$ initially decreases. At $\lambda=U$, the critical intrac-
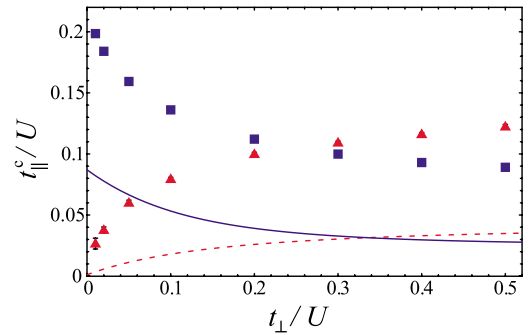
FIG. 3. (Color online) Critical intrachain hopping $t_{\parallel}^{c}$ as a function of $t_{\perp}$ for symmetric double wells ($\lambda=0$). Dashed and solid lines represent $t_{\parallel}^{c}$ for the half- and unit-filling MI phases calculated within the PMFA. Triangles and squares represent $t_{\parallel}^{c}$'s for the half- and unit-filling MI phases calculated by the infinite TEBD method.
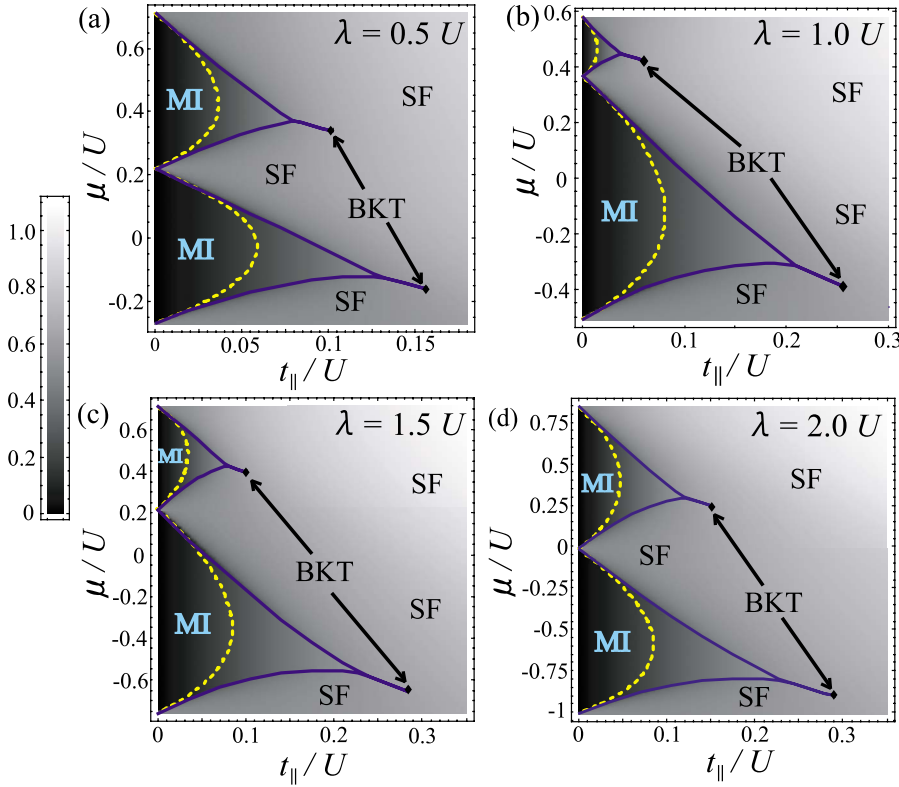
FIG. 4. (Color online) Phase diagrams for tilted double wells ($t_\perp = 0.1U$).

hain hopping reaches a minimum at which $t_\parallel^c \simeq \sqrt{2} t_\perp / 6$, since the states $|1,1\rangle$ and $|0,2\rangle$ are nearly degenerate, i.e., the local state of the MI phase at $\lambda = U$ is $|\Phi_{2,0}\rangle \simeq (|1,1\rangle + |0,2\rangle)/\sqrt{2}$. The development of this local coherence then pushes the system into the SF phase. Further increase of λ moves the system away from this degeneracy which favors SF, and forces $t_\parallel^c$ to increase, causing a reentrance into a MI phase. In particular, when $\lambda \gg U$, all atoms move to a single chain and are in $|0,2\rangle$; thus the critical value becomes $t_\parallel^c \simeq (5 - 2\sqrt{6})U/2$, as expected for a single chain [16].

The nonmonotonic behavior of $t_\parallel^c$ shows a reentrant quantum phase transition from MI to SF to MI, induced by the tilt λ, when $t_\parallel^c$ is kept between $(t_\parallel^c)_{min}$ and $(t_\parallel^c)_{max}$. Taking into account the high degree of control achieved in double-well optical lattices [5], we expect the reentrant transition to be observed experimentally. However, since we do not expect
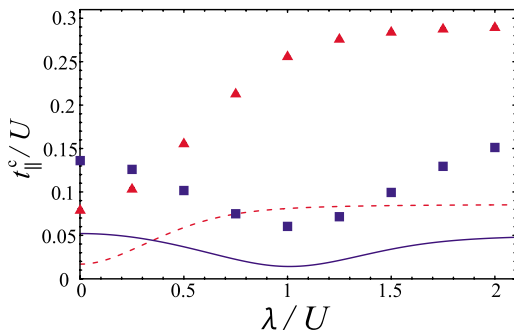
FIG. 5. (Color online) Critical values $t_\parallel^c$ of the intrachain hopping as a function of λ for fixed value of the interchain hopping $t_\perp = 0.1U$. (Error bars are smaller than the size of the symbols.)

the PMFA to give quantitatively correct results for the double-well (ladder) optical lattice, we next discuss numerical results using the TEBD method.

B. TEBD approach

In order to determine quantitatively the phase diagrams for double-well (ladder) optical lattices, we use the infinite-size version of TEBD [10], which provides an excellent ground state for 1D quantum lattice systems via imaginary time evolution. In order to apply the TEBD method to our problem, we map the double-well (ladder) Bose-Hubbard model into a single chain with *next-nearest-neighbor* hopping, whose ground state can be calculated via the *swapping* technique [18]. We note that the infinite TEBD algorithm has been recently applied to single chains with only *nearest-neighbor* hopping, where the quantum Berezinskii-Kosterlitz-Thouless critical point was obtained for the unit-filling case [19]. While the maximum number of bosons per site is $N_{max} = \infty$, convergence is already achieved in our numerical calculations when $N_{max} = 4$ for $\nu = 1/2$ and $N_{max} = 5$ for $\nu = 1$.

The phase diagrams in the $(\mu, t_\parallel)$ plane are shown in Figs. 2 and 4, where the solid lines indicate the MI-SF phase boundaries, which have roughly a triangular shape. At the sides of the MI lobe, the phase transition occurs from a $\nu = 1/2, 1$ MI to a SF with $\nu \neq 1/2, 1$. However, the two sides of the "triangle" merge for each MI phase (see dots in Figs. 2 and 4), producing a phase transition from a $\nu = 1/2, 1$ MI to a SF with $\nu = 1/2, 1$, which is of the BKT type [17,20].

In order to locate the phase boundaries we calculate directly the mean number of atoms per double well, $\tilde{n}$
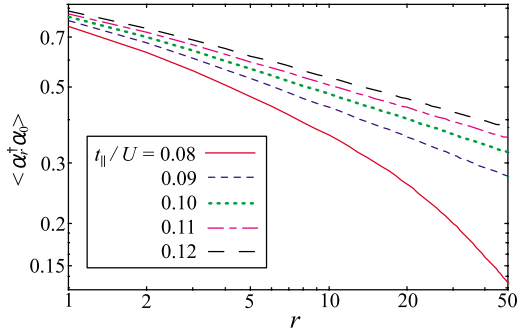
FIG. 6. (Color online) Correlation function $\langle \hat{\alpha}_r^\dagger \hat{\alpha}_0 \rangle$ as a function of the intrachain hopping $t_\parallel$, where $t_\perp = 0.2U$, $\lambda = 0$, and $\nu = 1/2$.

FIG. 7. (Color online) Exponent K extracted for four intervals, where $t_\perp = 0.2U$, $\lambda = 0$, and $\nu = 1/2$. The dashed line represents $K = K_c$ (=1/2) line.

$\equiv \Sigma_\eta \langle \hat{n}_{i,\eta} \rangle$, which is integer in the MI regions. We also calculate the fluctuation $\sigma \equiv \sqrt{\langle \hat{n}_i^2 \rangle - \langle \hat{n}_i \rangle^2}$, which is small deep in the MI regions, and relatively large in the SF regions. The fluctuation σ is represented by density plots in the phase diagrams of Figs. 2 and 4. Since we are interested in local observables, such as $\tilde{n}$ and σ, convergence is already achieved for $\chi = 15$, where χ is the size of the basis set retained in the TEBD procedure [9].

We locate the BKT transition on the lines of integer $\tilde{n}$ ($\nu = 1/2, 1$) by calculating the correlation function $\langle \hat{\alpha}_r^\dagger \hat{\alpha}_0 \rangle$, where $\hat{\alpha}_i^\dagger$ creates an atom in the lowest single-particle state of a double well. The SF phase of the double-well ladder can be regarded as a two-band Tomonaga-Luttinger liquid (TLL), and the correlation function exhibits power-law decay as $\langle \hat{\alpha}_r^\dagger \hat{\alpha}_0 \rangle \propto r^{-K/2}$. The exponents K_c at the phase transitions can be calculated from the TLL theory. For instance, when $\max(t_\perp, \lambda) \gg U$, our system is effectively a single 1D chain and has the critical value $K_c = 1/2$ for the BKT transition [17]. In addition, when $\lambda = 0$ and $\tilde{n} = 2(\nu = 1)$, the critical value is also $K_c = 1/2$ [20]. Consequently we use the criterion $K_c = 1/2$ to identify the critical point for the BKT transition at integer values $\tilde{n}(\nu = 1/2, 1)$.

In Fig. 6, the correlation function $\langle \hat{\alpha}_r^\dagger \hat{\alpha}_0 \rangle$ (in logarithmic scale) is shown as a function of the intrachain hopping $t_\parallel$, for $t_\perp = 0.2U$, $\lambda = 0$, and $\nu = 1/2$. We can see that $\langle \hat{\alpha}_r^\dagger \hat{\alpha}_0 \rangle$ indeed has power-law behavior proportional to $r^{-K/2}$ for sufficiently large $t_\parallel$. For instance, see the dashed line in Fig. 6 corresponding to $t_\parallel/U = 0.12$. In contrast, deep in the MI regime the correlation function does not exhibit power-law behavior, but an exponential decay (see the solid line in Fig. 6 corresponding to $t_\parallel/U = 0.08$).

In Fig. 7, we plot the exponent K as a function of $t_\parallel$, for $t_\perp = 0.2U$, $\lambda = 0$, and $\nu = 1/2$. The exponent K is obtained by fitting the function $f(r) = ar^{-K/2}$, with free parameters a and K, to the correlation function $\langle \hat{\alpha}_r^\dagger \hat{\alpha}_0 \rangle$ shown in Fig. 6. To achieve a high-precision value for K, we use the TEBD method with a large size for the basis set ($\chi = 60$). We use the intervals $10 \leqslant r \leqslant 15$, $15 \leqslant r \leqslant 20$, $20 \leqslant r \leqslant 25$, and $25 \leqslant r \leqslant 30$ for the fit and take the average value of K for each interval to produce error bars. The critical intrachain hopping $t_\parallel^c$ along the lines of integer $\tilde{n}$ is determined by taking the
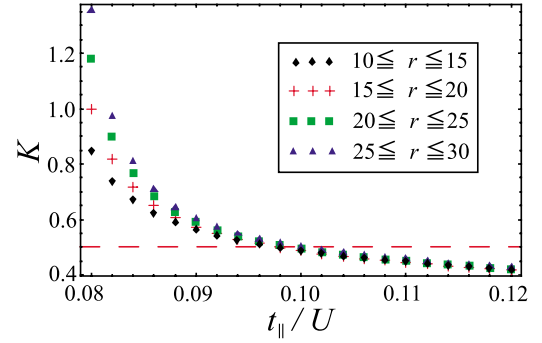
intersection of $K(t_\parallel/U)$ and $K = K_c = 1/2$. The dots in Figs. 2 and 4 correspond to the BKT transition points calculated via the TEBD method. In Figs. 3 and 5, the critical values $t_\parallel^c$ obtained via TEBD are shown as triangles and squares for $\tilde{n} = 1, 2$ ($\nu = 1/2, 1$), respectively. The phase boundaries asymptotically approach those of the PMFA as $t_\parallel$ tends to zero. On the other hand, differences between the PMFA and TEBD results are significant when $t_\parallel$ is relatively large. In particular, the values of $t_\parallel^c$ obtained using TEBD are more than twice as large as those obtained within the PMFA. Furthermore, the general form of the phase boundaries in the $(\mu, t_\parallel)$ plane is triangular for TEBD, while is it rounded for the PMFA. However, the qualitative behavior of the phase diagram as a function of $t_\perp$ and λ obtained within the PMFA is consistent with that of the TEBD method.

V. CONCLUSION

In summary, we have studied the superfluid-to-Mott insulator transition of bosons in double-well (ladder) optical lattices. Applying the time-evolving block decimation method to the two-legged Bose-Hubbard model, we have calculated the zero-temperature phase diagram. We have found that the phase diagram changes significantly depending on the interchain hopping and tilt of the double wells. In particular, we have shown that the tilt can be used to induce reentrant transitions between Mott insulator and superfluid phases. Through a comparison of the results of TEBD and the perturbative mean-field approach, we have shown that the PMFA captures some qualitative trends, but fails to describe the phase diagram quantitatively. Especially, the PMFA fails dramatically in obtaining the critical points for the Berezinskii-Kosterlitz-Thouless transition between the Mott-insulator and superfluid phases at commensurate fillings, while TEBD provides an accurate location for these critical points.

[1] D. Jaksch and P. Zoller, Ann. Phys. (N.Y.) **315**, 52 (2005).

[2] M. Greiner, O. Mandel, T. Esslinger, T. W. Hänsch, and I. Bloch, Nature (London) **415**, 39 (2002).

[3] I. B. Spielman, W. D. Phillips, and J. V. Porto, Phys. Rev. Lett. **98**, 080404 (2007).

[4] T. Stöferle, H. Moritz, C. Schori, M. Köhl, and T. Esslinger, Phys. Rev. Lett. **92**, 130403 (2004).

[5] J. Sebby-Strabley, M. Anderlini, P. S. Jessen, and J. V. Porto, Phys. Rev. A **73**, 033605 (2006).

[6] D. C. Johnston, J. W. Johnson, D. P. Goshorn, and A. J. Jacobson, Phys. Rev. B **35**, 219 (1987).

[7] M. Azuma, Z. Hiroi, M. Takano, K. Ishida, and Y. Kitaoka, Phys. Rev. Lett. **73**, 3463 (1994).

[8] E. Dagotto, Rep. Prog. Phys. **62**, 1525 (1999).

[9] G. Vidal, Phys. Rev. Lett. **91**, 147902 (2003); **93**, 040502 (2004).

[10] G. Vidal, Phys. Rev. Lett. **98**, 070201 (2007).

[11] M. P. A. Fisher, P. B. Weichman, G. Grinstein, and D. S. Fisher, Phys. Rev. B **40**, 546 (1989).

[12] P. Buonsante, V. Penna, and A. Vezzani, Phys. Rev. A **72**, 031602(R) (2005).

[13] P. Buonsante and A. Vezzani, Phys. Rev. A **70**, 033608 (2004).

[14] A. M. Rey, I. I. Satija, and C. W. Clark, New J. Phys. **8**, 155 (2006).

[15] V. G. Rousseau, D. P. Arovas, M. Rigol, F. Hébert, G. G. Batrouni, and R. T. Scalettar, Phys. Rev. B **73**, 174516 (2006).

[16] D. van Oosten, P. van der Straten, and H. T. C. Stoof, Phys. Rev. A **63**, 053601 (2001).

[17] T. D. Kühner, S. R. White, and H. Monien, Phys. Rev. B **61**, 12474 (2000).

[18] Y.-Y. Shi, L.-M. Duan, and G. Vidal, Phys. Rev. A **74**, 022320 (2006).

[19] J. Zakrzewski and D. Delande, e-print arXiv:cond-mat/0701739.

[20] P. Donohue and T. Giamarchi, Phys. Rev. B **63**, 180508(R) (2001).